

Electronic structure of a potential optical crystal $\text{YBa}_3\text{B}_9\text{O}_{18}$: Experiment and theory

Z. H. Zhang,¹ Jianjun Yang,² Ming He,¹ X. F. Wang,¹ and Quan Li^{1,a)}

¹Department of Physics, The Chinese University of Hong Kong, Shatin, New Territory, Hong Kong

²Department of Physics and Engineering Physics, University of Saskatchewan, Saskatoon, Canada S7N 5E2

(Received 20 February 2008; accepted 10 April 2008; published online 28 April 2008)

Using valence electron energy loss spectroscopy and *ab initio* band structure calculations, we have studied the basic electronic structure of a potential optical crystal $\text{YBa}_3\text{B}_9\text{O}_{18}$. Its optical band gap E_g is experimentally estimated as 6.3 eV and the origins of the individual interband transitions have been identified. In addition, the theoretical calculation reveals the strong anisotropic characteristic of the material band structure, accounting for its large birefringence. © 2008 American Institute of Physics. [DOI: 10.1063/1.2918131]

The recent discoveries of a series of new isostructural rare earth and alkaline earth borate compounds, $\text{REBa}_3\text{B}_9\text{O}_{18}$ (RE=Y, Pr, Nd, Sm, Eu, Gd, Tb, Dy, Ho, Er, Tm, and Yb) have aroused great research interest due to their rich varieties in structure, wide transmittance spectra, wide band gaps, and many interesting optical properties.¹ The strong anisotropy makes the birefringence of this series of crystals to be about 0.12, which is comparable to that of the β - BaB_2O_4 crystal,² making them especially promising in a number of optical applications such as liquid crystal displays, light modulators, color filters, wave plates, and optical axis gratings. Among these families of materials, $\text{YBa}_3\text{B}_9\text{O}_{18}$ is an interesting one. Unlike many other rare earth and alkaline earth borates, the centrosymmetrical structure of $\text{YBa}_3\text{B}_9\text{O}_{18}$ determines its zero value of the even rank nonlinear optical susceptibility. Nevertheless, its large birefringence, together with the excellent scintillation property (as revealed by the x-ray excited luminescence measurement),³ the chemical stability, and the relatively low fabrication cost make $\text{YBa}_3\text{B}_9\text{O}_{18}$ an attractive optical crystal.

Understanding the basic electronic structure of $\text{YBa}_3\text{B}_9\text{O}_{18}$ is critical in interpreting its optical behavior as well as predicting other physical properties. In the present study, we have employed both valence electron energy loss spectroscopy (VEELS) and first-principle calculations to investigate the electronic structure of this recently discovered crystal. While VEELS provides information on the collective free-electron oscillations as well as single electron excitations from the valence band (VB) to the empty density of states in the conduction band (CB),⁴ the first-principle calculation is adopted to predict the electronic and structural properties of the same materials.⁵ The combination of experimental and theoretical approaches reveals the basic electronic structure characteristics of $\text{YBa}_3\text{B}_9\text{O}_{18}$, including the material band gap, the individual interband transitions, as well as its anisotropic band structure.

$\text{YBa}_3\text{B}_9\text{O}_{18}$ single crystals grown by the Czochralski method³ were used in our studies. High resolution images were obtained by using the transmission electron microscope (TEM) (Tecnai 20ST, FEG). VEELS experiments were carried out by using a Gatan imaging filtering system attached to the same microscope. The energy loss spectra were ac-

quired at zero-momentum transfer. The zero loss peak of the raw spectrum was first removed by using routine procedures established in literatures,⁶⁻⁹ followed by a Fourier-log deconvolution to eliminate contribution from the plural scattering, and generate the material loss function ($\text{Im}[-(1/\epsilon(\omega))]$). Theoretical calculations were based on density functional theory using the Vienna *ab initio* simulation package (VASP).¹⁰⁻¹³ The crystal structure parameters of $\text{YBa}_3\text{B}_9\text{O}_{18}$ was obtained from the experimental results,¹ with optimization on the lattice parameters ($a=7.1841 \text{ \AA}$ and $c=16.9283 \text{ \AA}$), which were used in all calculations.

$\text{YBa}_3\text{B}_9\text{O}_{18}$ adopts a space group $P6_3/m$ and each B atom is bonded to three O atoms to form BO_3 groups, the three of which further constitute a planar hexagonal B_3O_6 ring.¹ These planar rings are stacked along the c axis in the unit cell, with regular YO_6 octahedral and irregular BaO_6 and BaO_9 polyhedra existing in between the hexagonal B_3O_6 rings. Such structural characteristic is clearly revealed by the high resolution TEM images shown in Figs. 1(a) and 1(b), which are taken along the [001] and [100] crystalline directions, respectively. The lattice constants obtained from the images agree well with those obtained from the XRD results.¹

The loss function of $\text{YBa}_3\text{B}_9\text{O}_{18}$ is shown in Fig. 2. We first discuss the band gap (E_g) determination. Erni and Browning⁹ have suggested that a power-law function can be simply used to locally fit the tail of the zero-loss peak. Consequently, the band gap of $\text{YBa}_3\text{B}_9\text{O}_{18}$ can be roughly estimated as $\sim 6.3 \text{ eV}$ by this method. Alternatively, fitting the edge-on slope of the loss function near the band gap using the $(E-E_g)^{0.5}$ for direct band gap and $(E-E_g)^{1.5}$ for indirect band gap material serves as a more precise method,¹⁴ which

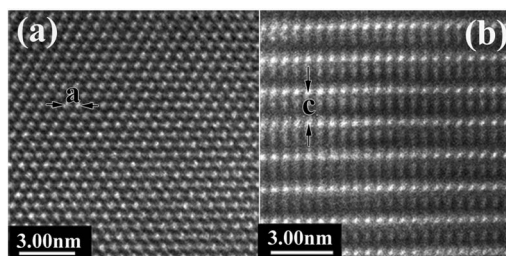


FIG. 1. High resolution TEM images of $\text{YBa}_3\text{B}_9\text{O}_{18}$, taken from (a) the [001] and (b) the [100] zone axes.

^{a)}Electronic mail: liquan@phy.cuhk.edu.hk.

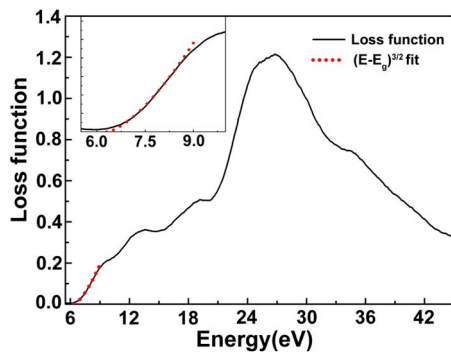


FIG. 2. (Color online) VEELS result of $\text{YBa}_3\text{B}_9\text{O}_{18}$. The inset shows the enlarged band gap region with fitting.

also suggests the nature of the material band gap (direct versus indirect). The $(E-E_g)^{1.5}$ curve generates a best fit for the experimental loss function (fitting result was shown as the dashed line in Fig. 2), leading to the determination of the band gap as ~ 6.3 eV, being consistent with the rough estimation using the power-law fit.

Above the band gap, there are five well-resolved peaks in the loss function, located at ~ 9.4 , ~ 13 , ~ 19.2 , ~ 26.2 , and ~ 34.6 eV, respectively. The dominant peak at 26.2 eV can be assigned to the bulk plasmon oscillation. The highly damped bulk plasmon peak is characterized by its large excitation cross sections for fast electrons. A brief estimation of the collective plasmon excitation with the Drude formula⁸ using the free-electron approximation also supports this assignment. Other peaks should originate from the single electron excitation from the VB to the empty density of states (DOS) in the CB, and their profiles are expected to have direct correlation with the joint DOS (JDOS) between occupied and unoccupied states in the energy bands.⁷

In order to interpret these individual transitions, we investigate the energy band structure of $\text{YBa}_3\text{B}_9\text{O}_{18}$ by using first-principle calculation [Fig. 3(a)]. The results are consis-

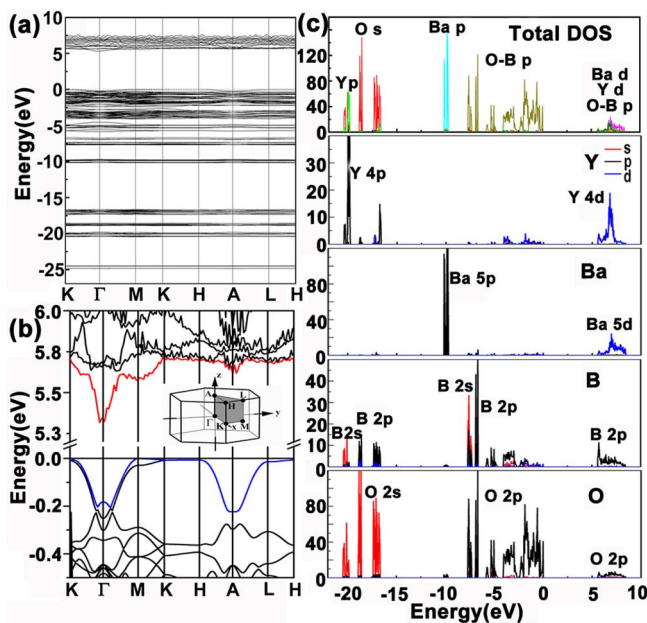


FIG. 3. (Color online) (a) The calculated energy band structure of $\text{YBa}_3\text{B}_9\text{O}_{18}$. (b) The enlarged energy band in the vicinity of the Fermi level, the inset illustrates the corresponding Brillion zone. (c) The calculated TDOS and PDOS results of $\text{YBa}_3\text{B}_9\text{O}_{18}$.

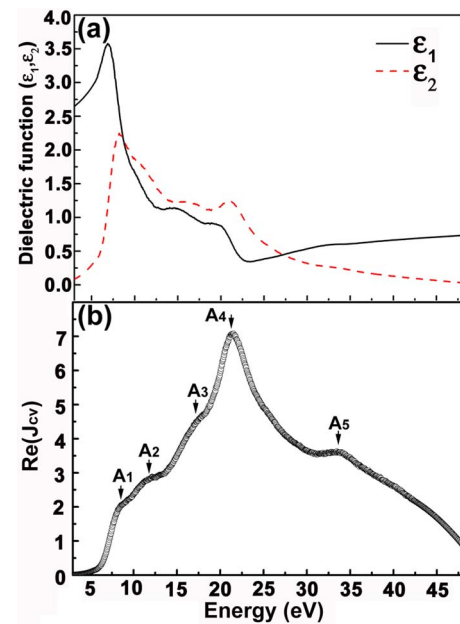


FIG. 4. (Color online) (a) The complex dielectric function (real part ϵ_1 , imaginary part ϵ_2). (b) The real part of $J_{CV}(E)$.

tent with those calculated using the CASTEP code by Duan *et al.*¹⁵ An enlarged band structure near the Fermi level is shown in Fig. 3(b) and the k -space direction reference of the corresponding Brillion zone is illustrated in the inset of Fig. 3(b). The calculated band diagram indicates that the CB minimum is at Γ point, while the VB maximum (VBM) is at M point, suggesting that $\text{YBa}_3\text{B}_9\text{O}_{18}$ is an indirect band gap insulating materials, which is consistent with the EELS results. Nevertheless, the calculated energy separation of the two points is ≈ 5.3 eV, which is lower than the measured band gap of ≈ 6.3 eV, that is likely due to the underestimation caused by the local density approximation calculations. The VBM is relatively flat (i.e., the hole with large effective mass) in the M to K and K to H directions drops sharply but (i.e., the hole with much smaller effective mass) in the M to Γ and K to Γ directions. Such anisotropy in the energy band leads to a reduction in the dimensionality of the optical response, which is the origin of its large birefringence. From the calculated partial DOS (PDOS) results [shown in Fig. 3(c)], the occupied states, from which interband transitions originate, are the Y 4p levels ranging from -21 to -17 eV, the Ba 5p levels at -10 eV, the B 2s levels at -20.5 and -7.5 eV, the B 2p levels spanning from -18.9 to -1.5 eV, the O 2s ranging from -21 to -16.8 eV, and the O 2p ranging from -7.6 to -0.15 eV. The most prominent unoccupied energy bands in the CB are composed of Y 4d (5.3 – 8.14 eV), Ba 5d (5.3 – 8.47 eV), B 2p (5.3 – 8.4 eV), as well as the O 2p levels (5.3 – 8.3 eV).

Now, we try to determine the origin of each interband transition observed in the EELS by comparing their energetics to the calculated total DOS (TDOS). The interband transition strength J_{CV} is defined as the convolution of the valence and CB DOS weighted by the dipole selection rule matrix elements and can be directly compared to the JDOS. Such a quantity can be deduced from the equation $J_{CV}(E) = (m_0^2/e^2\hbar^2)(E^2/8\pi^2)[\epsilon_2(E) + i\epsilon_1(E)]$, given that the dielectric function $\epsilon(\omega)$ is obtained from the material loss function $\text{Im}[-1/\epsilon(\omega)]$ via the Kramers–Kronig analysis. For com-

TABLE I. Correspondence of the interband transition energetics between the experimental and theoretical results.

Transition	Energy (eV)	Predominant orbital character
A ₁	8.3	O–B 2 <i>p</i> –Y 4 <i>d</i> , Ba 5 <i>d</i>
A ₂	11.5	O–B 2 <i>p</i> –Y 4 <i>d</i> , Ba 5 <i>d</i> ; B 2 <i>s</i> –O 2 <i>p</i>
A ₃	16.9	Ba 5 <i>p</i> –Y 4 <i>d</i>
A ₄	21.4	Ba 5 <i>p</i> –Y 4 <i>d</i>
A ₅	33.7	Y 4 <i>p</i> , B 2 <i>p</i> , O 2 <i>s</i> -higher CBs ^a

^aCBs=conduction bands.

putational convenience, the prefactor $m_0^2 e^{-2\hbar^{-2}}$ was taken to be unity so that the $J_{CV}(E)$ spectra plotted in this work have a unit of eV^2 instead of the unit of density. By using simple algebraic transformations, other optical parameters can be obtained. The obtained dielectric function (real part ϵ_1 , imaginary part ϵ_2) and the real part of $J_{CV}(E)$ are shown in Figs. 4(a) and 4(b), respectively.

Several prominent interband transition features are observed in Fig. 4(b). All of the features can be referenced to its band structure characteristics. Based on the analysis of the calculated TDOS, the first feature located at ~ 8.3 eV in the $J_{CV}(E)$ was mainly attributed to the transitions between the O–B 2*p* electrons into the Y 4*d* and the Ba 5*d* levels in the CBs. The second feature centered at ~ 11.5 eV agrees with the characteristic of the O–B 2*p* to the Y 4*d* transition, while the Ba 5*d* and the B 2*s* to the O 2*p* transitions also make contributions to such a peak as justified from the PDOS. The third and fourth peaks at ≈ 16.9 and ~ 21.4 eV correspond to excitations from the Ba 5*p* to the Y 4*d* level, and a fifth feature, occurring at much higher energy (≈ 33.7 eV), is likely to rise from the excitations from the Y 4*p*, B 2*p*, and O 2*s* levels to the higher DOS in the CBs. For convenience, the predominant orbital characteristics are given in Table I.

In conclusion, the electronic structure of a potential optical crystal $\text{YBa}_3\text{B}_9\text{O}_{18}$ was analyzed by using both electron

energy loss spectroscopy and *ab initio* band structure calculations. The E_g of this indirect band gap material is determined as ~ 6.3 eV from the VEELS data, which also lead to the deduction of the dielectric function of this new compound. The band structure calculation of the material suggests a strong anisotropic characteristic associated with its electronic structure and, thus, possible optical response. Assignments of the individual interband transitions have been accomplished by comparing the interband transition energy to the *ab initio* calculated PDOS. The combination of experimental and theoretical approaches leads to a thorough understanding on the electronic structure of $\text{YBa}_3\text{B}_9\text{O}_{18}$.

The authors acknowledge the financial support by grants from the research grant council of HKSAR (Project No. CUHK 402105) and direct grant under Project No. 2060317.

¹X. Z. Li, C. Wang, X. L. Chen, H. Li, L. S. Jia, L. Wu, Y. X. Du, and Y. P. Xu, *Inorg. Chem.* **43**, 8555 (2004).

²J. Friebe, K. Moldenhauer, E. M. Rasel, W. Ertmer, L. Isaenko, A. Yelisseyev, and J.-J. Zondy, *Opt. Commun.* **261**, 300 (2006).

³Ming He, X. L. Chen, Y. P. Sun, J. Liu, J. T. Zhao, and C. J. Duan, *Cryst. Growth Des.* **7**, 199 (2007).

⁴R. F. Egerton, *Electron Energy Loss Spectroscopy in the Electron Microscope* (Plenum, New York, 1986).

⁵Y. N. Xu, P. Rulis, and W. Y. Ching, *Phys. Rev. B* **72**, 113101 (2005).

⁶B. Rafferty, S. Pennycook, and L. Brown, *J. Electron Microsc.* **49**, 517 (2000).

⁷K. van Benthem, C. Elsässer, and R. H. Frencze, *J. Appl. Phys.* **90**, 6156 (2001).

⁸S. Lazar, G. Botton, M.-Y. Wu, F. Tichelaar, and H. Zandbergen, *Ultramicroscopy* **96**, 535 (2003).

⁹R. Erni and N. D. Browning, *Ultramicroscopy* **104**, 176 (2005).

¹⁰J. P. Perdew, J. A. Chevary, S. H. Vosko, Koblar A. Jackson, Mark R. Pederson, D. J. Singh, and C. Fiolhais, *Phys. Rev. B* **46**, 6671 (1992).

¹¹G. Kresse and J. Joubert, *Phys. Rev. B* **59**, 1758 (1999).

¹²G. Kresse and J. Furthmüller, *Phys. Rev. B* **54**, 11169 (1996).

¹³G. Kresse and J. Hafner, *Phys. Rev. B* **47**, 558 (1993).

¹⁴B. Rafferty and L. M. Brown, *Phys. Rev. B* **58**, 10326 (1998).

¹⁵C. Duan, X. Wang, and J. Zhao, *J. Appl. Phys.* **101**, 023501 (2007).